Effect of Oxide Powders on Austenitic Stainless-Steel Welding by Active GTAW Process

Gurveen Singh* and Dinesh Kumar Shukla
Department of Mechanical Engineering
Dr. B.R. Ambedkar National Institute of Technology,
Jalandhar, Punjab, India
*gurveensingh03@gmail.com

Received: *27.03.2018,* ***Accepted:*** *22.05.2018*

Abstract

This paper enunciates the effect of six different oxide powders (SiO_2, ZnO, SeO_2, CdO_2, Fe_2O_3 and CuO) applied as a surface active element to austenitic stainless steel SS-304 grade welded by Gas Tungsten arc welding (GTAW) process. Weld bead geometry, Microstructure, Ferrite content, Microhardness, and Arc column shape, X-Ray diffraction were analyzed for the different oxide powders in GTAW process. As Oxygen is known to be a surface active element for austenitic stainless steels, its presence in the weld region can increase the weld bead depth and alter other metallurgical and mechanical properties of fusion zone. Experiment results corroborated that the oxide powders can drastically increase the weld bead penetration. Microstructure and ferrite content varies for the welded austenitic stainless steel with different oxide flux powders. Arc column becomes constricted in the presence of oxide powders leads to increase in weld bead penetration. Micro-hardness of the weldments also increases in most of the oxide powders thereby improving mechanical properties.

Keywords- Surface active flux, Weld bead geometry, Arc Constriction, Marangoni convection, GTAW Process, Austenitic stainless steel.

Introduction

Gas tungsten arc welding (GTAW) uses a non-consumable tungsten electrode to produce the electric arc for heat required to fuse the materials together. The process is also termed as Tungsten inert gas (TIG) welding process. The electrode is covered with a concentric layer of inert gas flowing surrounding it to protect it from atmospheric contamination at high temperature. Autogenous welds can be made with GTAW process wherein the joint is made without using any filler wire (Tseng, 2013). It is a well-known process for high-quality joining of mild steel, stainless steel, aluminum, magnesium and their alloys with a huge application in the fabrication industry (Kuo, 2011). However while welding thick ferrous materials, due to the lack of penetration of the process, multi-pass welds are to be made for complete fusion of joint (Lu, 2004). V-Grooves are generally prepared in the material before welding to ensure full depth fusion for thick ferrous materials. This preparation of V-grooves and thereby multi-pass welding procedure leads to reduced productivity. There is a need for penetration improvement in the process so that thick materials can be welded in a single pass (Vidyarthy, 2016).

Several techniques have been implemented in past to improve the productivity of TIG welding. Active Flux assistance in GTAW process is one of the technique which can lead to increase in penetration and thereby increase the productivity of the process (Dhandha, 2015). Paton Welding Institute, Ukraine was first to propose the application of active flux (Modenesi, 2015). In this process, a flux powder containing oxide, chloride or fluoride is mixed with some thinner like acetone or ethanol and applied on the work-piece before welding as shown in Figure 1 (Tseng, 2012). The presence of flux compounds in the weld area can increase the penetration by reversing the Marangoni convection or surface tension driven flow of molten pool as illustrated in Figure 2 (Lu, 2009b). Previous works (Sambherao, 2013) had confirmed the increase in weld bead penetration based on Marangoni convection flow but still the results of few of the researchers were contradictory with each other. Hence in this paper, an attempt has been made to explore the effect of six different oxide powders (SiO_2, ZnO, SeO_2, CdO_2, Fe_2O_3 and CuO) on weld bead geometry, Microstructure, Micro-hardness, Ferrite Content and Arc column shape on SS-304 grade austenitic stainless steel welded with GTAW Process.

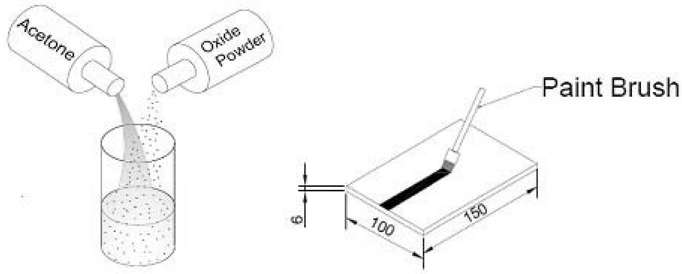

Figure 1: Application of Active flux

a) Mixing b) Coating

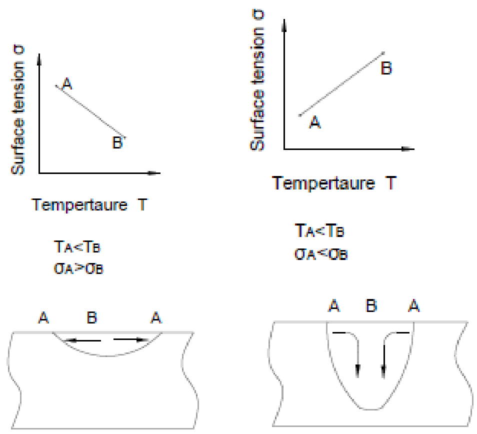

Figure 2: Reversal of surface tension with and without flux (Lu 2009a)

a) Without Flux, b) With Flux

Austenitic stainless steel SS-304 grade was selected for this study is most commonly used a grade of stainless steel. The percentage of alloying elements in SS-304 grade is given in Table-1. The test specimen plates were prepared with the size of 100 x 150 mm with 6mm thickness. Before welding, the surface of SS-304 grade plates was cleaned with a coarse abrasive paper and cleaned with acetone. All the oxide compounds were available in powder form. To prepare active flux, oxide powders were mixed with acetone in equal ratio to have a paint-like consistency and were applied to the surface of weld bead region prior to welding.

Table 1: Chemical Composition of SS-304

Element	**C**	**Cr**	**Ni**	**P**	**S**	**Mo**	**Si**	**Co**	**Cu**	**Mn**	**Fe**
%age	0.069	18.8	8.02	0.0341	0.0103	0.242	0.312	0.106	0.434	0.985	Balance

A TIG welding machine power source (EWM-Tetrix 351) was used with an automated system in which the specimen can be moved at a stabilized speed while keeping the torch fixed. A constant value of 180 Amps direct current was used with negative electrode polarity. A water-cooled torch with 2% thoriated tungsten electrode of diameter 2.4 mm was used in this study. Electrode vertex angle of 30^0, Electrode to workpiece distance of 2mm and electrode extension of 3 mm was kept fixed for all experiments. Argon was selected as the inert gas to protect the weld region from atmospheric contaminations and its flow rate was fixed at 7 LPM.

Active flux suspension was prepared by mixing one of the oxide powders with acetone. As such, six different oxide powders (SiO_2, ZnO, SeO_2, CdO, Fe_2O_3 and CuO) were used to prepare six different active flux suspensions. The active flux suspensions were applied with a paint brush to the weld area of the plate before welding. The acetone being a volatile liquid vaporizes quickly leaving behind the powder stuck with the base metal. Autogenous bead on plate weld was made in a single pass at 180 A welding current and 2mm/s welding speed keeping all welding variables identical. The constant welding parameters are listed in Table-2.

Table 2: Constant Welding parameters for experimentation

S. No.	Parameter	Value
1	Current	180A
2	Speed	2mm/s
3	Electrode gap	2mm
4	Polarity	DCEN
5	Electrode type	Thoriated 2%
6	Electrode Dia	2.4 mm
7	Electrode vertex angle	30 degrees
8	Electrode extension	3-4 mm
9	Inert Gas used	Pure Argon
10	Shielding Gas Flow rate	7LPM

The welded samples were sectioned in the transverse direction and metallographic specimens were prepared by grinding and polishing the specimen. Etching was done by dipping the specimen in a solution of HCl, $CuSO_4$ and distilled water. The weld bead cross-sections were photographed by Leica Microscope at different magnifications. Micro-hardness of the specimens was measured by Vickers hardness testing machine. A camera was used to capture the video of arc column while welding.

Results and Discussions

a) Weld Bead Geometry

Weld cross sections of samples welded with different flux compositions were photographed and the bead measurements were recorded with Tool Makers Microscope. Table 3 shows the values of weld bead penetration and width of weld samples made with different flux powders and without flux as well.

As per past research work, the reversal of surface tension driven flow significantly affects in improving the weld bead profile. While TIG welding with the application of SiO_2, ZnO and CdO flux, the temperature coefficient of surface tension on the liquid pool transformed from a negative to a positive value. The surface tension at the mid of weld region becomes greater than at the weld pool edge. The liquid stream of the molten pool effectively changes direction and flows from the weld pool edge to the middle, and downward. The outcome demonstrated that utilizing SiO_2, ZnO and CdO flux powders made a huge increment in weld depth and synchronous reduction in weld pool width. More than 140% increase in penetration has been recorded while using these flux powders as a surface active element. The wide and shallow fusion zone shape changed to narrow and deep while using these flux powders. CuO Powder has also shown more than 100% increase in penetration. Whereas the effect of Selenium dioxide and Ferric Oxide powders on penetration were not that much significant. This was due to the fact that during welding with SeO_2 and Fe_2O_3, the welding arc was inconsistent and had shown some spatter. Hence, the welding arc was not constricted and lead to poor penetration thereby. Figure 3 represents the bar chart with the values of weld bead width and depth of penetration and Figure 4 shows the weld bead profile obtained by using different oxide powders.

Table 3: Weld Bead dimensions with different oxide powders at 180A

Exp. No.	Flux Used	Penetration (mm)	Width (mm)	Aspect ratio	%age increase in penetration
1	Silicon Dioxide(SiO_2)	5.61	7.34	0.76	157%
2	Zinc Oxide (ZnO)	5.21	6.36	0.82	140%
3	Selenium Dioxide(SeO_2)	3.21	8.96	0.31	47%
4	Cadmium Oxide (CdO)	5.46	6.4	0.85	150%
5	Ferric Oxide(Fe_2O_3)	3.15	10.62	0.28	43%
6	Cupric Oxide (CuO)	4.55	6.15	0.74	108%
7	Without Flux	2.18	10.74	0.21	NA

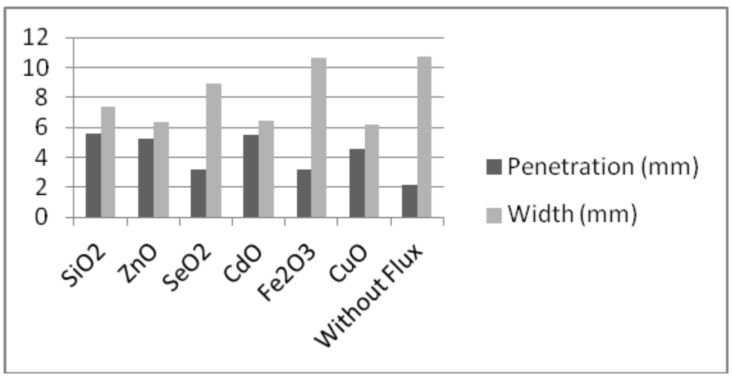

Figure 3: Bar chart showing comparative values of weld bead penetration and width.

b) Effect on bead surface appearance

Figure 4 shows the weld bead surface appearance of the welds made with different flux powders. The residues of chemical powders applied can be seen in all cases. However, the residues can be cleaned with a fine wire brush and cloth dipped in acetone. The bead appearance of SiO_2 powder is much better as compared to other chemical powders. The bead appearance of ZnO, CdO, and CuO is also satisfactory after cleaning. The beads appearance of welds made with using SeO_2 Powder shows porosity and blow holes and even the bead prepared was not smooth. Weld bead prepared using Fe_2O_3 powder was not satisfactory. The arc was not stable while welding with SeO_2 and Fe_2O_3 powders leading to poor bead surface appearance.

c) Effect on Microstructure and Ferrite Content

The microstructure of the specimens was analyzed by using Leica Microscope. Figure 5 shows the microstructure of different welds obtained at the same magnification. After welding, due to high cooling rates, the weld metal zone exhibits the skeletal ferrite and lathy ferrite formation in austenite microstructure resulting from primary ferrite solidification. The retained ferrite content in the welded samples was determined by Leica Phase expert application and presented in Table 4 and Figure 6. Without flux, weld sample has exhibited maximum ferrite content of 29%. The samples welded with oxide powders articulated the reduction of ferrite content. The minimum ferrite content was observed in specimen welded with the application of selenium oxide powder. The reduction of ferrite content can be related to the increased heat flux due to arc constriction and reversal of Marangoni convection in presence of oxide powders. The increased heat input increases the cooling rates also. Under increased solidification conditions, undercooling of dendrite tip increases stabilizes austenite more as compared to ferrite as the major phase of solidification. The preferred solidification phase will be the one with highest dendrite tip temperature at a given growth rate. Thus, as growth rate increases, austenite becomes preferred over ferrite. (John C. Lippold 2005) Thus it can be concluded that the use of oxide powders increases the heat flux owing to increased solidification rates. Increased solidification rates promote the formation of austenite rather than ferrite. Thus all the samples welded with oxide powders exhibit reduced ferrite content.

S.No.	Powder Used	Powder Appearance	Surface appearance after welding	Weld Bead Profile obtained
1.	Silicon Dioxide (SiO_2)		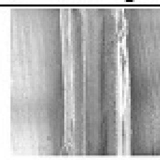	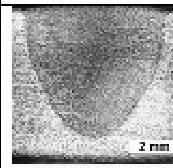
2.	Zinc Oxide (ZnO)	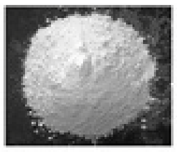	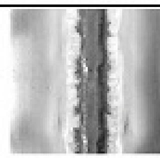	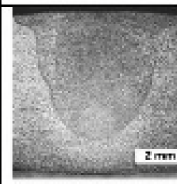
3.	Selenium Oxide (SeO_2)	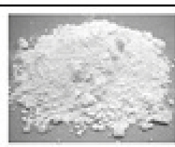	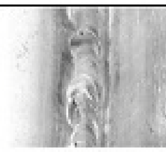	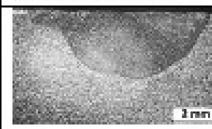
4.	Cadmium Oxide (CdO)		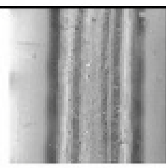	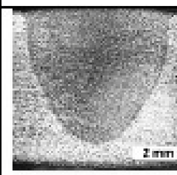
5.	Ferric Oxide (Fe_2O_3)	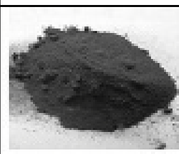	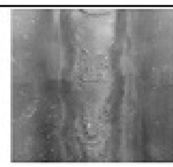	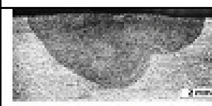
6.	Cupric Oxide (CuO)	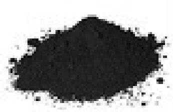	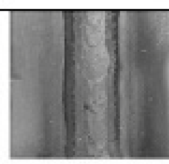	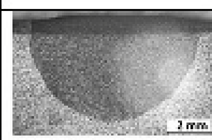
7.	Without Flux	NA	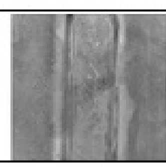	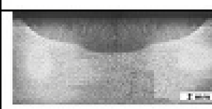

Figure 4: Weld bead surface appearance and weld bead profile of samples welded with different oxide powders.

Table 4: Ferrite percentages for samples welded with different oxide powders

Exp. No.	Flux Used	Average Ferrite Content(%age)
1	Silicon Dioxide(SiO_2)	26.64
2	Zinc Oxide (ZnO)	24.93
3	Selenium Dioxide(SeO_2)	20.28
4	Cadmium Oxide (CdO)	22.41
5	Ferric Oxide(Fe_2O_3)	24.78
6	Cupric Oxide (CuO)	25.18
7	Without Flux	29.02

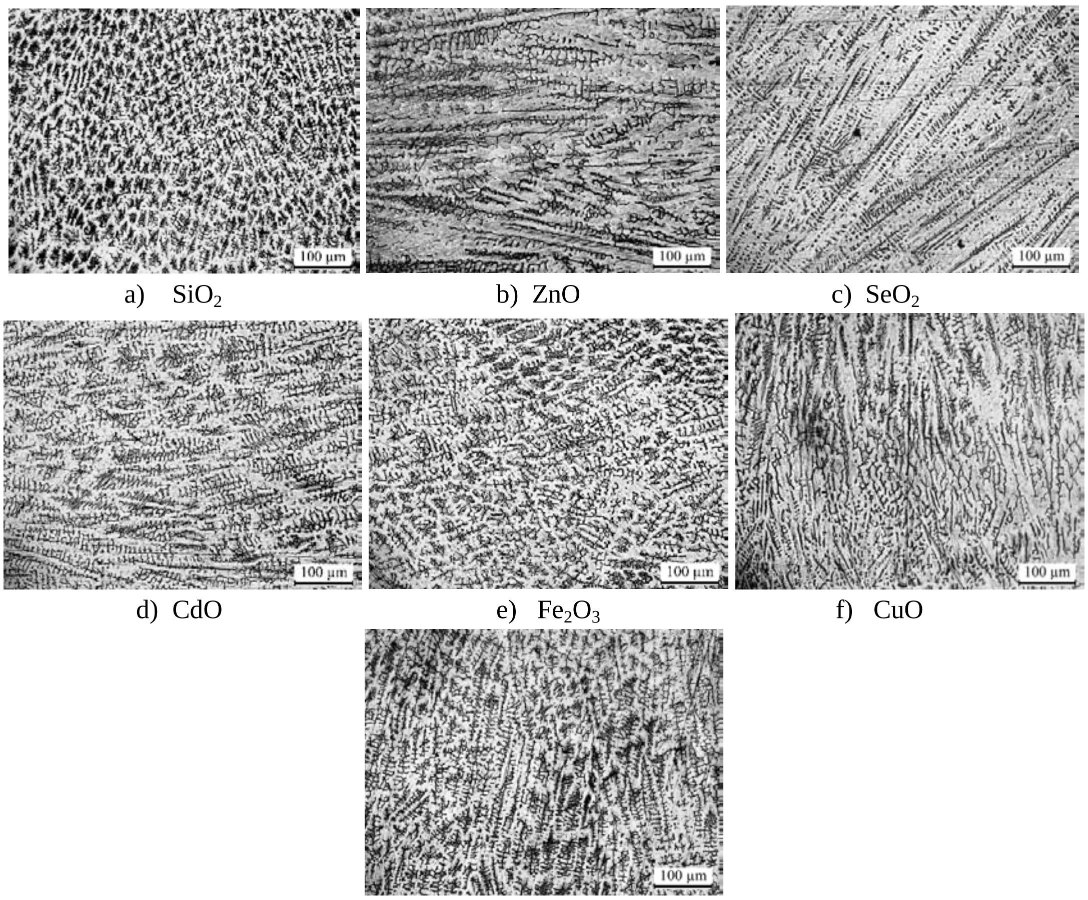

a) SiO_2 b) ZnO c) SeO_2

d) CdO e) Fe_2O_3 f) CuO

g) Without Flux

Figure 5: Microstructure of samples welded with different oxide powders.

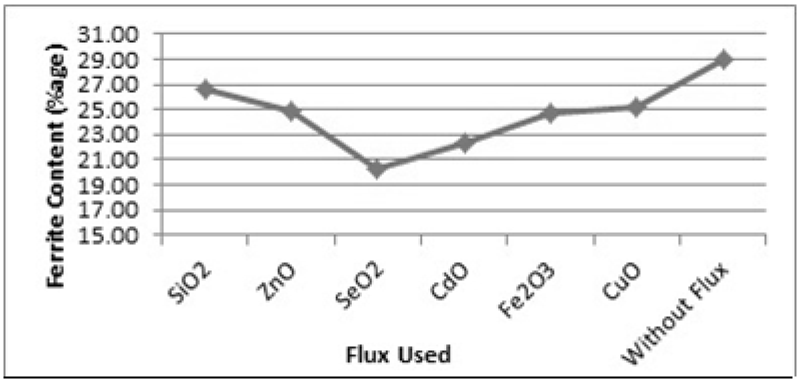

Figure 6: Bar chart showing values of ferrite percentage at fusion zone

d) Effect on Micro-hardness

Figure 7 shows the micro-hardness values of weld beads prepared using different oxide powders. Micro-hardness values were recorded at an interval of 0.5 mm and up to a distance of 5mm from both the sides of bead center to investigate the hardness profile of the bead area, heat affected zone and base metal. Microhardness values were measured by applying a load of 200 gm with a dwell period of 12 seconds. Average micro-hardness value of weld bead prepared with the application of SiO_2 powders was recorded as highest (219.5 HV) followed by bead prepared with ZnO flux powder (212.6 HV). It was further followed by SeO_2, CdO, and Fe_2O_3 with the average hardness value of the weld bead as 200.8 HV, 187.2 HV and 182.2 HV respectively. The hardness values of CuO powder were recorded with least value (170.7HV) even less than that of bead prepared without flux (178.5 HV). The average Hardness value of Base Metal without welding is 205 HV. Welding with SiO_2 and ZnO flux powders have recorded higher hardness values than that of base metal. This will further improve the mechanical properties of the welds prepared by these flux powders.

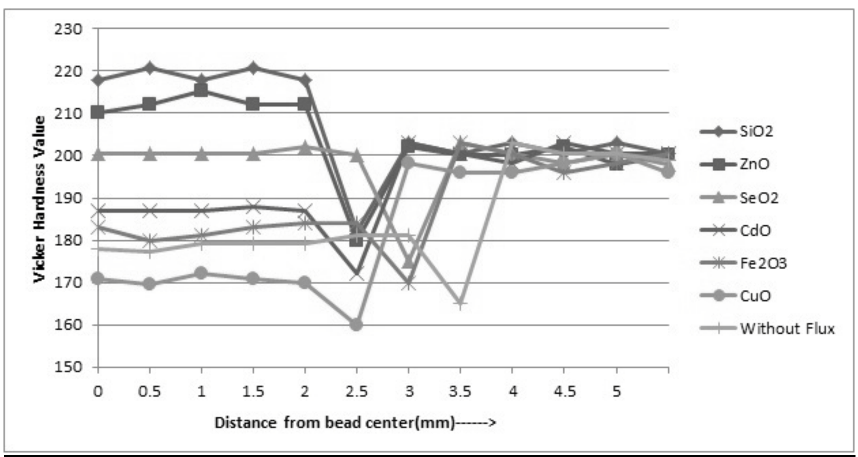

Figure 7: Effect of Oxide powders on hardness distribution profile

e) Effect of Flux on Arc Column

Figure 8 shows the recorded arc column of the weld during different oxide powders. While welding without flux, the arc column shape is wide and shallow thereby leading to poor penetration. TIG welding using active flux powders like SiO_2 and ZnO, the column becomes constricted. Arc constriction reduces the plasma column diameter and thus the anode area is reduced. The constricted arc increases the heat flux and arc force at anode region and leads to rise in temperature at the center of the weld pool. The increased heat density and temperature leads to a deeper flow of molten metal in the weld pool thereby increasing penetration.

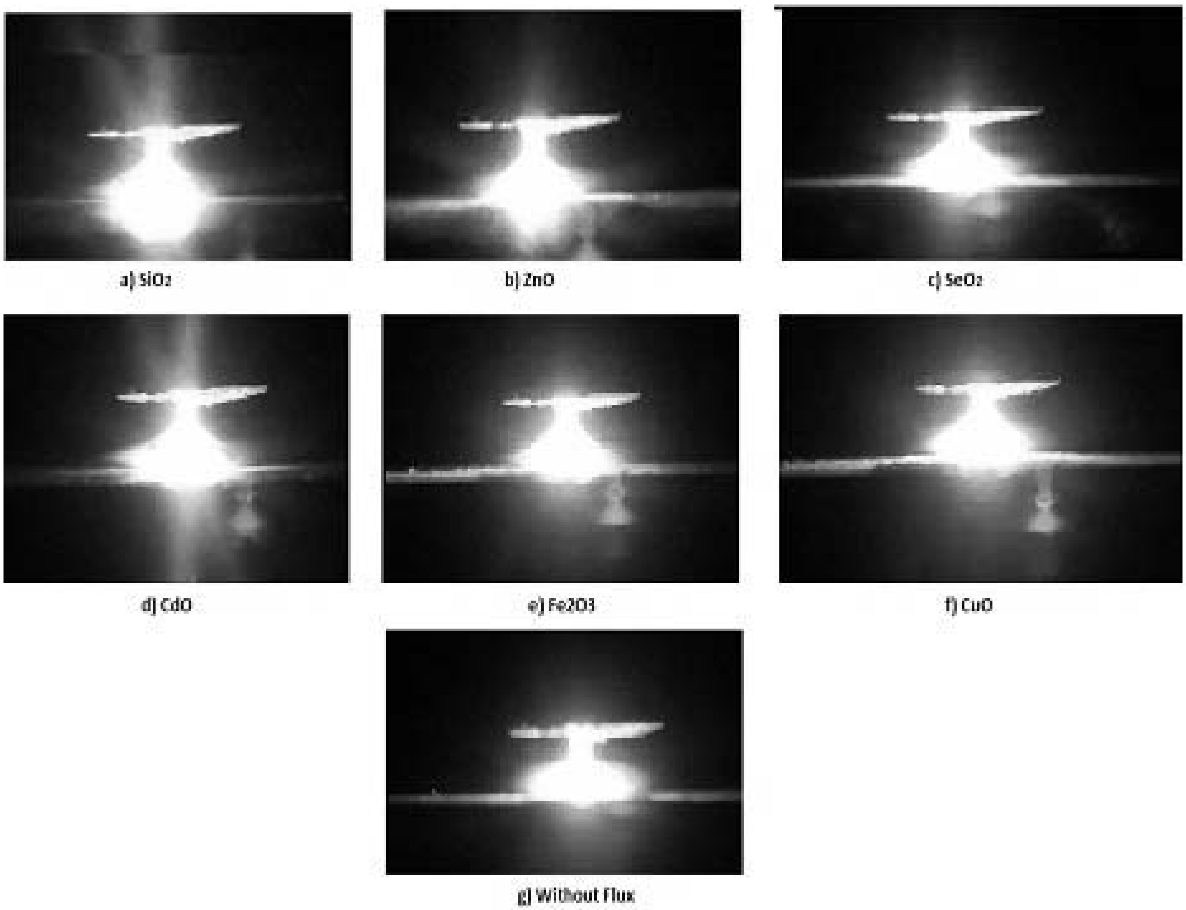

Figure 8: Arc column of sample welded with different oxide powders

In the plasma column, the electron interaction occurs at the outer peripheral part. When flux is applied, the oxygen ions of the flux and arc electrons interact to redistribute charger carriers and leads to the constriction of arc column(Tathgir et al. 2015). This constriction of arc column increased the energy flux and thereby the arc temperature. This phenomenon will increase the Lorentz force to promote a downward flow of molten metal. The included angle of the arc column was measured to confirm the above phenomenon. Table 5 shows the measured arc column angle for different oxide powders. The included angle of arc column obtained while welding without flux was 130^0. Whereas those obtained with the addition of oxide powders were recorded between 90^0 and 100^0. This confirms the arc constriction by using oxide powders. This constriction of the arc is reported to be the major phenomenon in increasing the weld bead penetration and reducing the weld bead width.

f) Material Characterization

X-Ray Diffraction (XRD) analysis was used to analyze the weld metal for any changes in phase formation and crystalline structure. XRD analysis was performed by a Cu target with generator settings at 40 mA, 45 kV. The data were collected in the range of 30^0 to 100^0 at a scan rate of 4 degrees per minute. Figure 9 shows the comparative plot of XRD patterns of different samples. Results show the presence of Austenite, Ferrite, Chromium Carbide, Iron-Chromium Oxide and Iron silicon in all the samples as indicated in Table 6 with their respective JCPDS reference number. XRD pattern of all the samples was almost same with peaks at the same position and of almost similar counts.

Table 5: Included Arc Angle obtained with different oxide powders

Exp. No.	Flux Used	Included Arc angle (Degrees)
1	Silicon Dioxide(SiO_2)	96^o
2	Zinc Oxide (ZnO)	94^o
3	Selenium Dioxide(SeO_2)	108^o
4	Cadmium Oxide (CdO)	95^o
5	Ferric Oxide(Fe_2O_3)	100^o
6	Cupric Oxide (CuO)	98^o
7	Without Flux	129^o

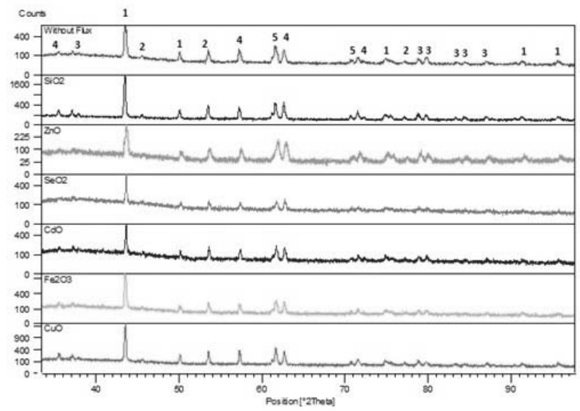

Figure 9: XRD pattern of weld beads using different oxide powders

Table 6: Data of peaks identified in XRD pattern

Compound	JCPDS No.	Number Allotted
Austenite	#330397	1
Ferrite	#030411	2
Chromium Carbide	#897244	3
$FeCr_2O_4$	#892618	4
FeSi	#860792	5

Conclusion

This paper presented the detailed experimental study to systematically investigate the effect of six different flux powders (SiO_2, ZnO, SeO_2, CdO, Fe_2O_3 and CuO) on weld bead geometry, bead appearance, microstructure, ferrite content, arc column behavior and microhardness values for GTA Welding of SS-304 grade material of 6 mm thickness. The results and conclusions can be summarized as below:

- SiO_2, ZnO and CdO oxide flux powders can improve the weld bead penetration by more than 140% as compared to that welded without flux. The welds made without flux were wide and shallow whereas the welds made with these flux powders were narrow and deep. CuO powder has also shown an increase in penetration. SeO_2 and Fe_2O_3 powders were not good in increasing the weld bead penetration.
- Bead surface appearance of the welds prepared by SiO_2, ZnO, CdO and CuO powders were satisfactory. Whereas surface of weld prepared by SeO_2 and Fe_2O_3 powders were not satisfactory.
- Use of oxide powders increases the heat flux owing to increased solidification rates. Increased solidification rates promote the formation of austenite rather than ferrite. All the samples welded with flux had shown lower ferrite content as compared to sample welded without flux.
- Arc Constriction was observed during welding with SiO_2 and ZnO flux powders. This arc constriction results from the electronegativity of ions of the active element present in weld pool.
- Microhardness at fusion zone of the welds prepared by SiO_2 and ZnO were highest followed by SeO_2, CdO, and Fe_2O_3. The Microhardness value of CuO Powder was least, even less than that of welded without flux.

Future Scope

This experimental study has been performed to explore the effect of six different oxide powders on GTA welding of austenitic stainless steel (SS-304). Results had shown that SiO_2 and ZnO flux powders can significantly improve the weld bead penetration and thereby productivity of the process. This outcome finds a huge application in fabrication industry like boilers manufacturing, structural components, container manufacturing etc. In future, this study can also be performed on some other materials, with some other kind of flux powders and may be with some other welding process also.

References

Dhandha, K.H, Badheka, V.J. 2015. Effect of activating fluxes on weld bead morphology of P91 steel bead-on-plate welds by flux assisted tungsten inert gas welding process. *Journal of Manufacturing Processes*,17, 48-57.

John, C. L., Damian, J. K. 2005. Welding Metallurgy and Weldability of Stainless Steels; *John Wiley & Sons Inc. Publications.*

Kuo, C.H., Tseng, K.H., Chou, C.P. 2011. Effect of Activated TIG Flux on Performance of Dissimilar Welds between Mild Steel and Stainless Steel. *Key Engineering Materials,* 479, 74–80.

Lu, S., Fujii, H., Nogi, K. 2004. Marangoni convection and weld shape variations in Ar-O2 and Ar-CO2 shielded GTA welding. *Materials Science and Engineering,* A 380, 290–297.

Lu, S., Fujii, H., Nogi, K. 2009a. Arc ignitability, bead protection and weld shape variations for He-Ar-O2 shielded GTA welding on SUS304 stainless steel. *Journal of Materials Processing Technology,* 209, 1231–1239.

Lu, S.P., Dong, W.C., Li, D.Z., Li, Y.Y. 2009b. Numerical simulation for welding pool and welding arc with variable active element and welding parameters. *Science and Technology of Welding and Joining,* 14, 509-516 .

Modenesi, P.J., Colen Neto, P., Roberto Apolinário, E., Batista Dias, K. 2015. Effect of flux density and the presence of additives in ATIG welding of austenitic stainless steel. *Welding International*, 29, 425–432 .

Sambherao, P.A.B. 2013. Use of Activated Flux For Increasing Penetration In Austenitic Stainless Steel While Performing GTAW. *International Journal of Emerging Technology and Advanced Engineering*, 3, 520–524.

Tathgir, S., Bhattacharya, A., Bera, T.K. 2015. Influence of Current and Shielding Gas in TiO_2 Flux Activated TIG Welding on Different Graded Steels. *Materials and Manufacturing Processes,* 30, 1115–1123.

Tseng, K.H., Chen, K.L. 2012. Comparisons Between TiO2- and SiO2-Flux Assisted TIG Welding Processes. *Journal of Nanoscience and Nanotechnology,* 12, 6359–6367.

Tseng, K.H. 2013. Development and application of oxide-based flux powder for tungsten inert gas welding of austenitic stainless steels. *Powder Technology*, 233, 72–79.

Vidyarthy, R.S., Dwivedi, D.K. 2016. Activating flux tungsten inert gas welding for enhanced weld penetration. *Journal of Manufacturing Processes*, 22, 211–228.